

Supramolecular Covalent Cellulose-based Bioplastics with High Transparency, Hydrophobicity, Ionic Conductivity, Mechanical Robustness and Recyclability

Quanfeng Liang, Mengqing Li, Yuchen Cao, Ren'ai Li* and Yunfeng Cao

Jiangsu Co-Innovation Center for Efficient Processing and Utilization of Forest Resources, Jiangsu Provincial Key Lab Pulp & Paper Science and Technology, Nanjing Forestry University, Nanjing 210037, P. R. China.

E-mail address: lirenai@njfu.edu.cn

Table S1. The component details and the appearances of diverse CBPs

Sample	Parameters (mass ratio)	Appearance
CBP-12	HDES:EC solution: LiTFSI:TPO =12:86:1:1	Transparency, rigid, tough
CBP-14	HDES:EC solution: LiTFSI:TPO =14:84:1:1	Transparency, tough
CBP-16	HDES:EC solution: LiTFSI:TPO =16:82:1:1	Transparency, soft

Note: The concentration of the EC solution was 5% and the solvent was DMF.

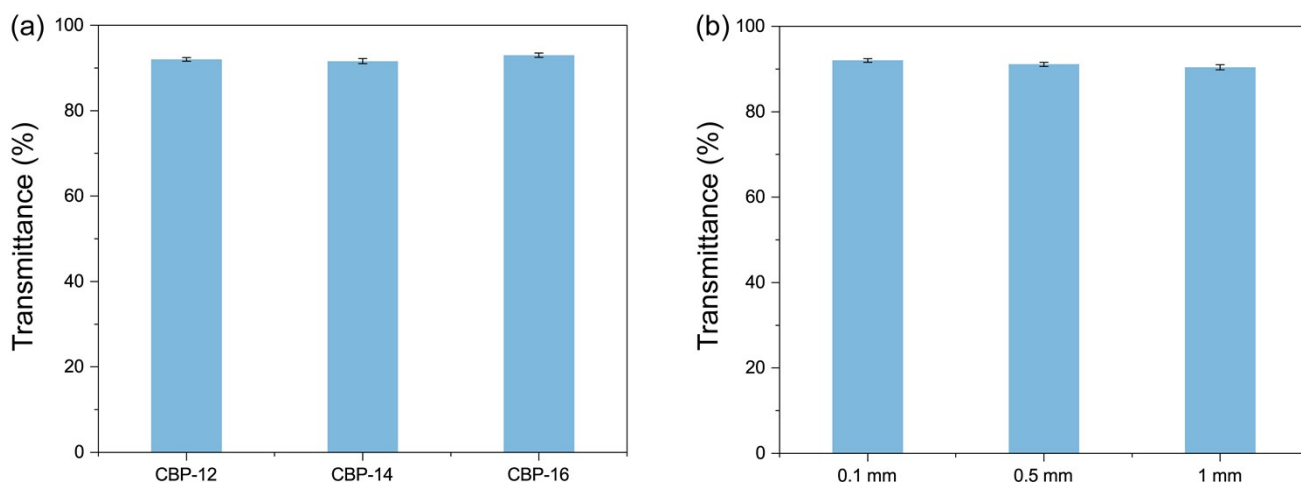


Figure S1. Optical transmittance of different CBPs samples and CBP-14 with different thicknesses

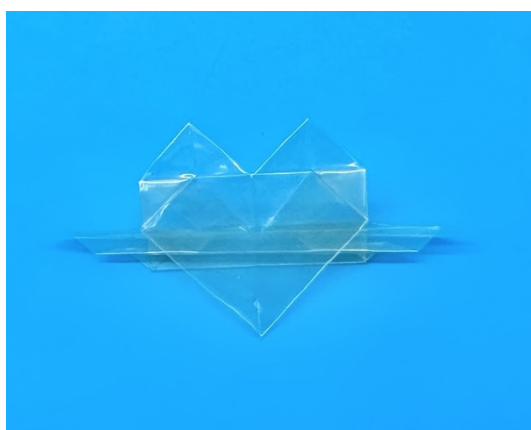


Figure S2. CBP can be folded into complex heart shapes, demonstrating its good flexibility.

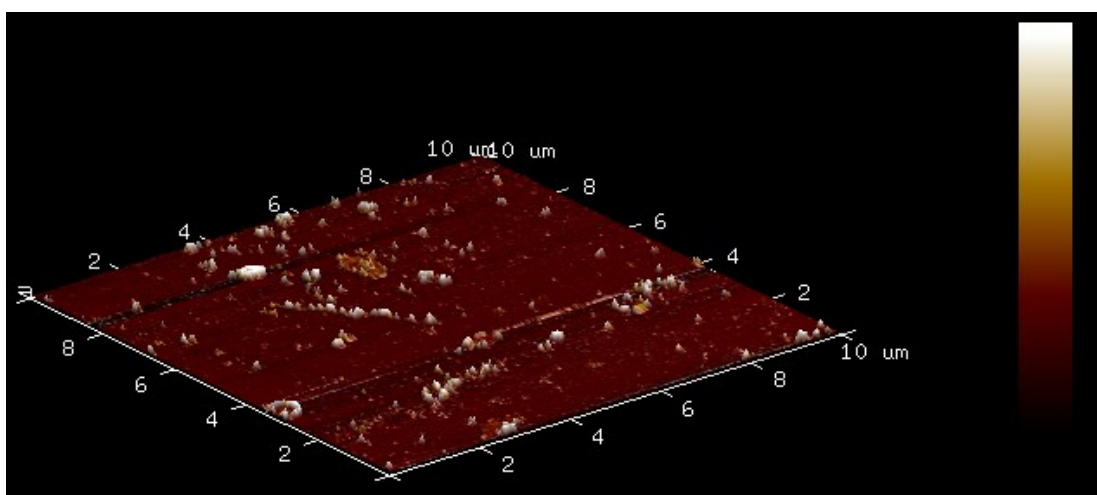


Figure S3. AFM phase diagram of CBP-16. The AFM phase image illustrated clear boundaries between hard (EC; bright spots) and soft (poly(HDES); dark zones) domains.

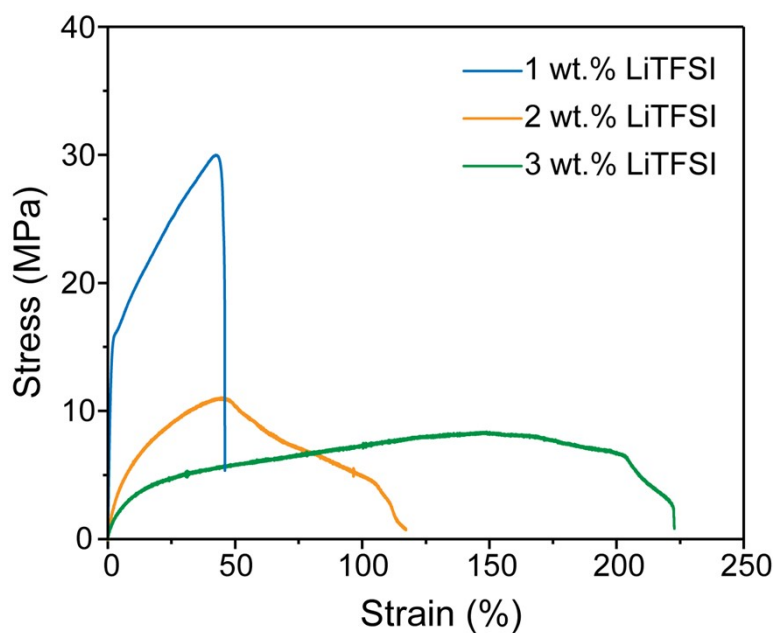


Figure S4. Stress-strain curves of CBPs containing different lithium salt contents.

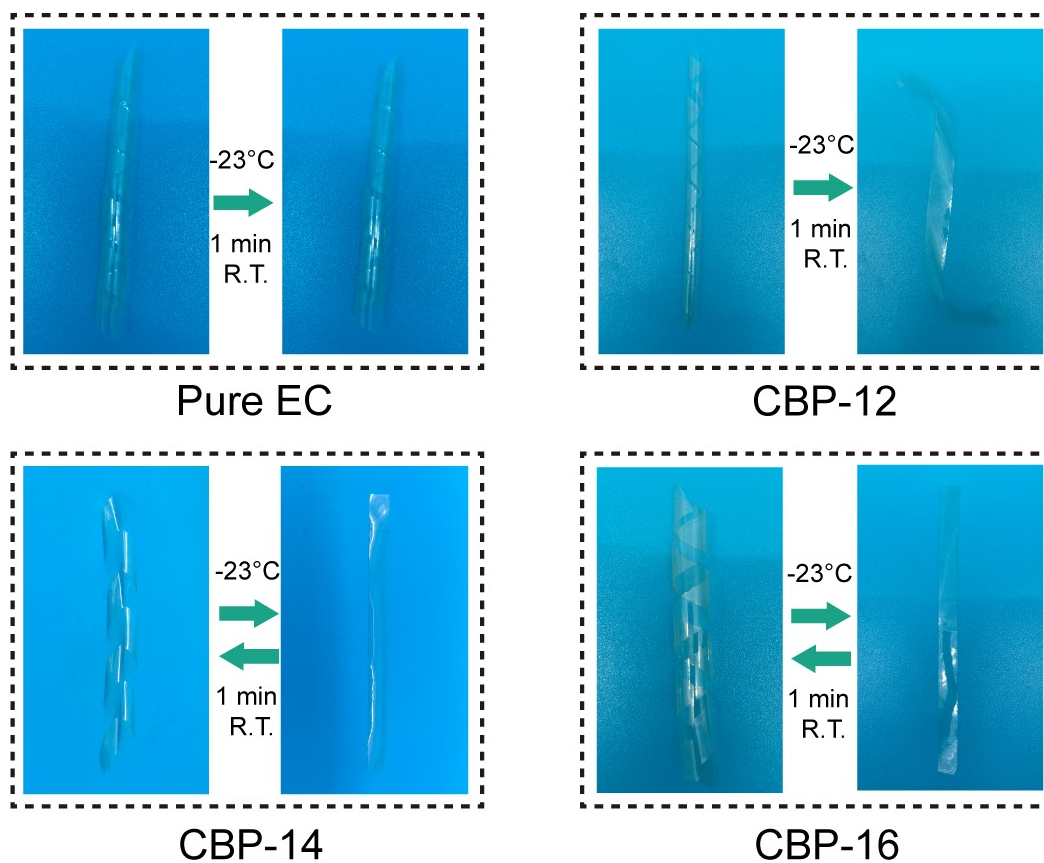


Figure S5. Comparison of shape memory function for pure EC and different CBPs.

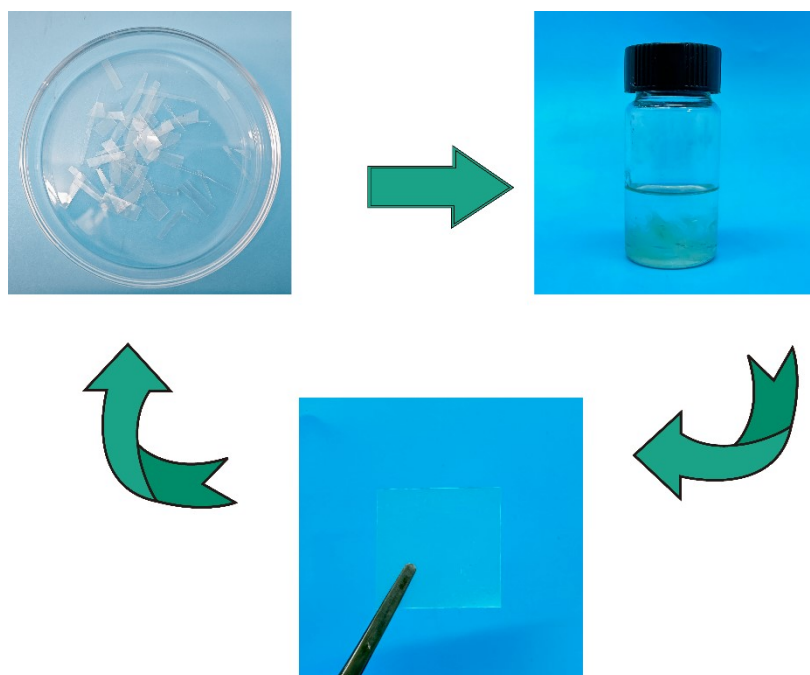


Figure S6. Using solvents (e.g. DMF) for CBP recycling at room temperature.

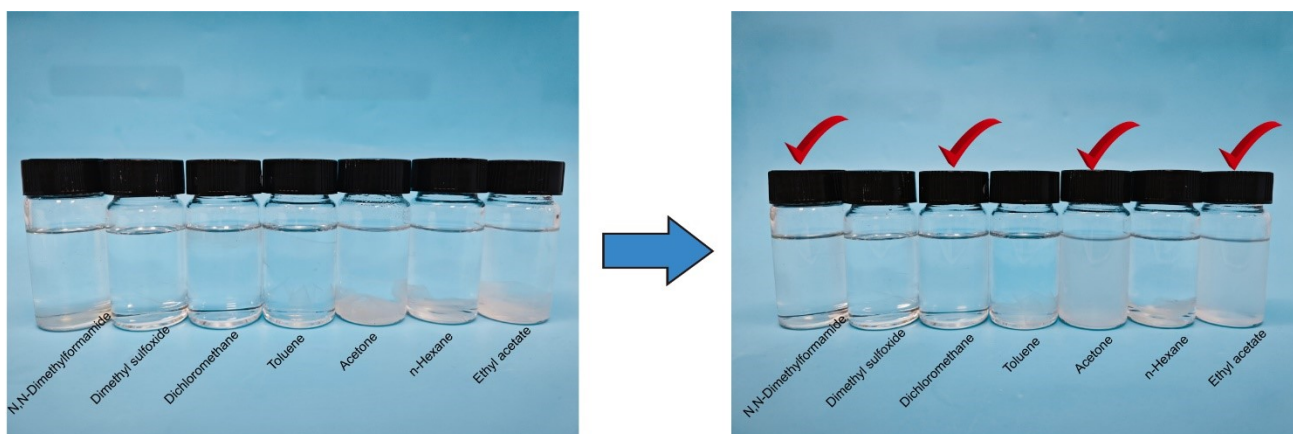


Figure S7. Solubility of CBP in different solvents such as dimethylformamide, dimethyl sulfoxide, dichloromethane, toluene, acetone, hexane and ethyl acetate.

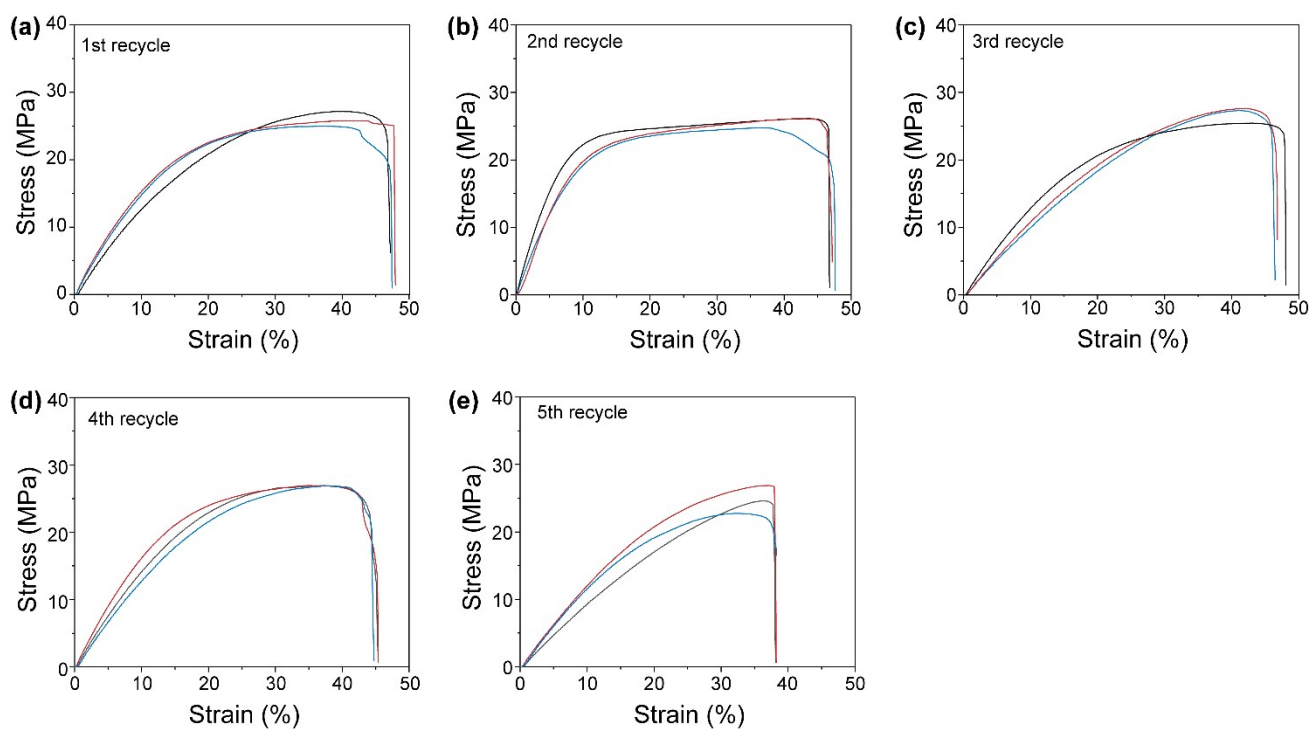


Figure S8. The stress-strain curve of CBP after recycling different times. Note: Each sample was tested 3 times. As shown, the samples maintained high tensile strength and flexibility after 5 recycling. However, the samples experienced a slight decrease in mechanical strength and stretchability after the 5th recycling compared to the first four cycles.

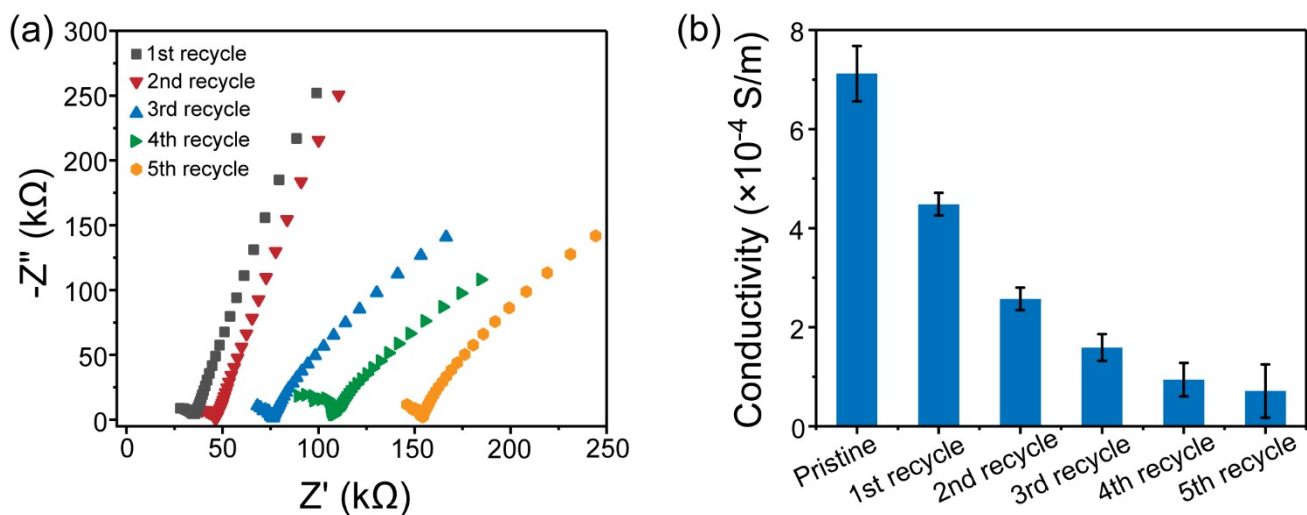


Figure S9. Electrochemical impedance spectra and ionic conductivities for CBPs with different recycles. As shown, CBP exhibited growing electrochemical impedance with decreasing ionic conductivity as the number of recycling times increased. This may be due to the fact that as the number of recycling increased, the CBP underwent degradation at the microscopic level, producing more low molecular weight compounds. This in turn caused an increase in the incompatibility among the system, leading to a decreased ionic conductivity.

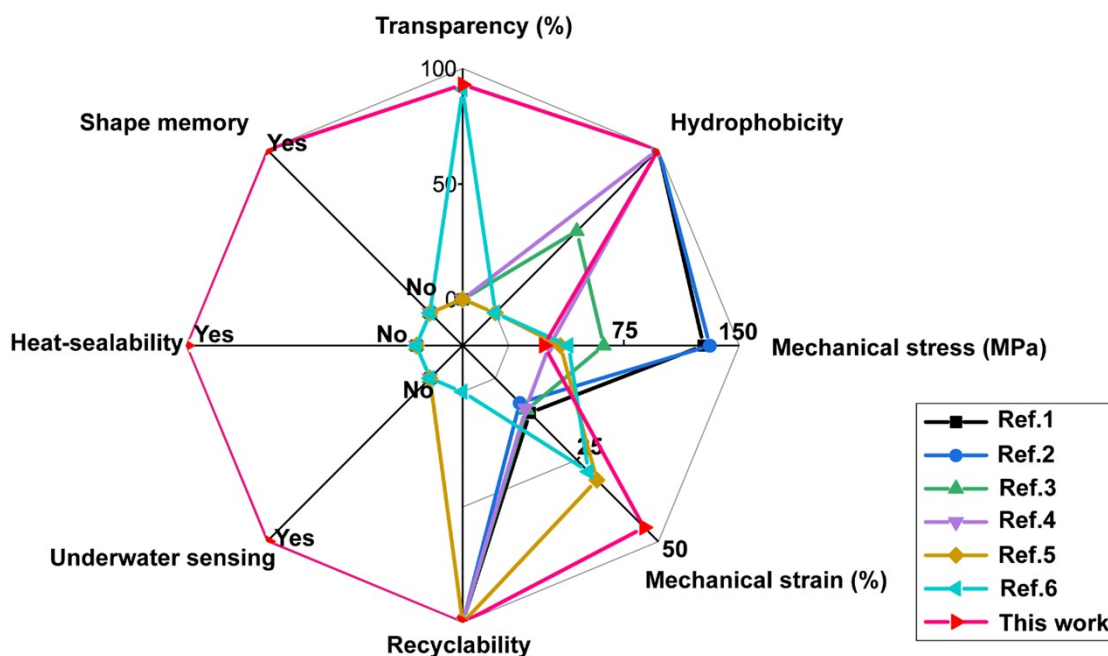


Figure S10. A comparison between this work and recently reported CBPs in terms of hydrophobicity, transparency, flexibility, stretchability, shape memory function, heat sealability, underwater sensing capability, and recyclability.

References

1. Q. Xia, C. Chen, Y. Yao, J. Li, S. He, Y. Zhou, T. Li, X. Pan, Y. Yao and L. Hu, *Nat. Sustain.*, 2021, **4**, 627-635.
2. S. Fang, X. Lyu, T. Tong, A. I. Lim, T. Li, J. Bao and Y. H. Hu, *Nat. Commun.*, 2023, **14**, 1203.
3. G. Zhou, H. Zhang, Z. Su, X. Zhang, H. Zhou, L. Yu, C. Chen and X. Wang, *Adv. Mater.*, 2023, **35**, 2301398.
4. Z. Su, L. Yu, L. Cui, G. Zhou, X. Zhang, X. Qiu, C. Chen and X. Wang, *ACS Nano*, 2023, DOI: 10.1021/acsnano.3c06175.
5. S. Zhang, Q. Fu, H. Li, P. Wu, G. I. N. Waterhouse, Y. Li and S. Ai, *Chem. Eng. J.*, 2023, **463**, 142452.
6. S. Guzman-Puyol, J. Hierrezuelo, J. J. Benítez, G. Tedeschi, J. M. Porras-Vázquez, A. Heredia, A. Athanassiou, D. Romero and J. A. Heredia-Guerrero, *Int. J. Biol. Macromol.*, 2022, **209**, 1985-1994.